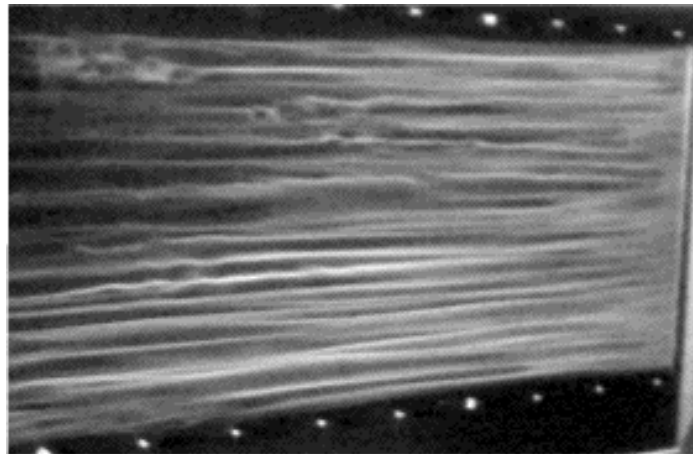




LARGE AMPLITUDE COHERENT STATES IN BOUNDARY LAYER

Alessandro Bottaro
DIAM, Università di Genova, Italy

Goal: identify stable/unstable, “*vortical states of motion*” in non-parallel boundary layers



Alfredsson & Matsubara, 1996

$U_\infty = 2 \text{ ms}^{-1}$ $Tu=6\%$

Based on joint work with:

S. Zuccher, P. Luchini, P. Andersson, L. Brandt, D.S. Henningson



Why *vortical states*?

Saffman (**ANYAS** 1983) holds that “*unstable quasi-steady vortical states probably exist in every flow*” and speculates that “*their shadows are present in the turbulent flow ... and that turbulence can be understood in term of their properties*”.

Current wisdom holds that a “small” set of *recurrent vortical patterns* is sufficient to develop predictive tools for non-equilibrium turbulent flows.

This idea has roots in the *prehistory* of chaos theory!

Lorenz attractor

(*J. Atmos. Sci.* 1963)

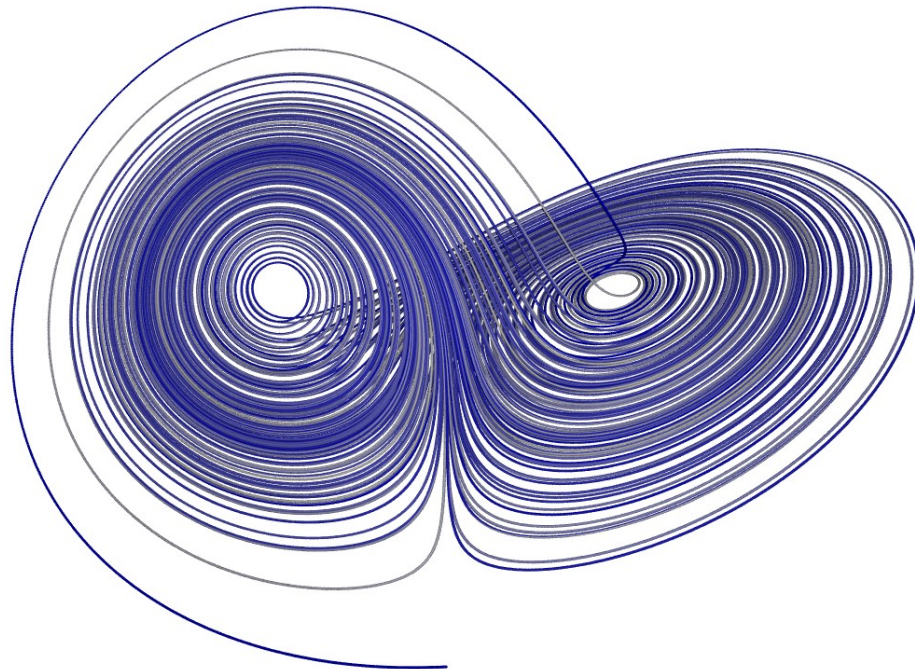
No steady states

No limit cycles

Sensitive dependence on IC

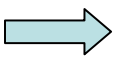


Local unpredictability





If turbulence can be interpreted as the wandering of the flow system's trajectory in phase space among **mutually repelling vortical states** (Cvitanović refers to this as *Hopf theory of chaos*) it may be possible to

1. identify the set of *vortical states* pertinent to each flow configuration and Reynolds number, &
2. compute sensible global averages ( **global** predictability) possibly retaining only the more *meaningful* patterns (i.e. the least unstable ones?)

Both tasks are difficult ...

(*cf.* Lan & Cvitanović, ***Phys. Rev E*** 2003, in the context of the 1D Kuramoto-Sivashinsky equation)



Success stories in the context of the Navier-Stokes equations

(chronological and incomplete ...)

6. Nagata (**JFM** 1990)

2. Ehrenstein & Koch (**JFM** 1991)

9. Cherhabili & Ehrenstein (**JFM** 1997)

10. Waleffe (**JFM** 2001, **PoF** 2003)

11. Kawahara & Kida (**JFM** 2001)

12. Faisst & Eckhardt (**PRL** 2003)

Wedin & Kerswell (**JFM** 2004)

Hof *et al.* (**Science** 2004, **PRL** 2005)

3D finite amplitude solutions
in plane Couette flow

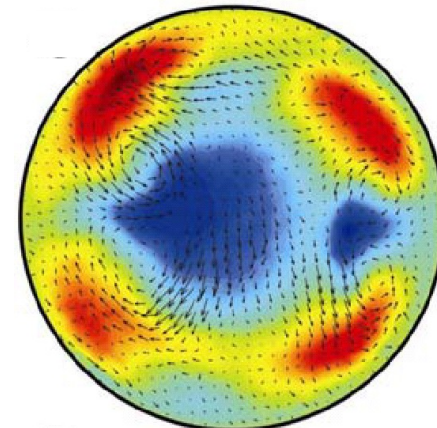
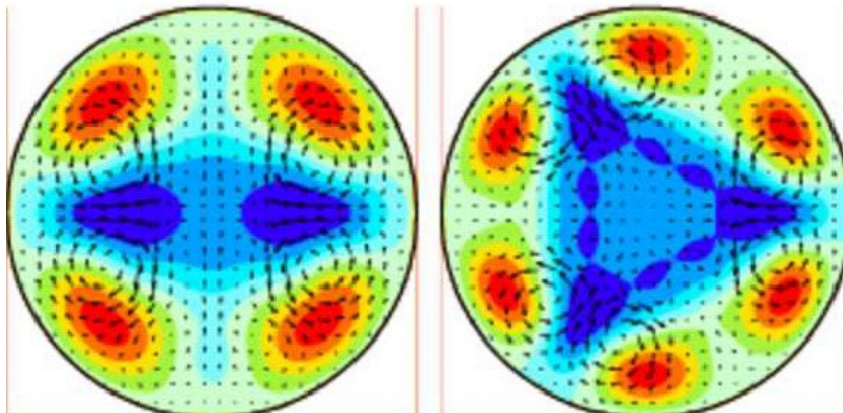
Poiseuille flow

plane Couette flow

plane Couette & Poiseuille
flows, self-sustaining process

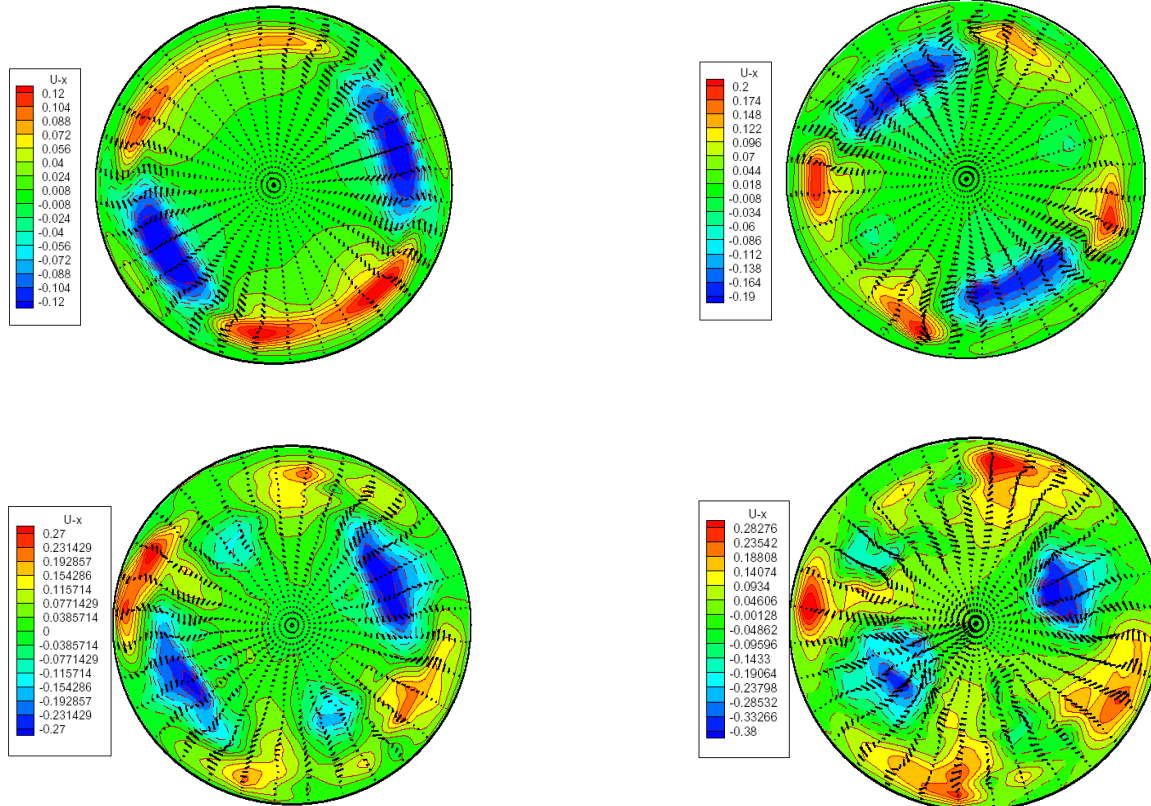
first numerical evidence of the
existence of unstable recurrent
patterns in Couette flow at $Re=400$

TW in pipe flow





Further confirmation as to the presence of recurrent patterns in pipe flow: Gavarini, Bottaro & Nieuwstadt, *JFM*, 2004 & *IUTAM Symposium*, Bristol, 2004



Vortices, streaks and *TW* sustain one another against viscous decay



Possibly, the square duct is “nicer” because of the presence of geometrical symmetries that constrain the flow ...

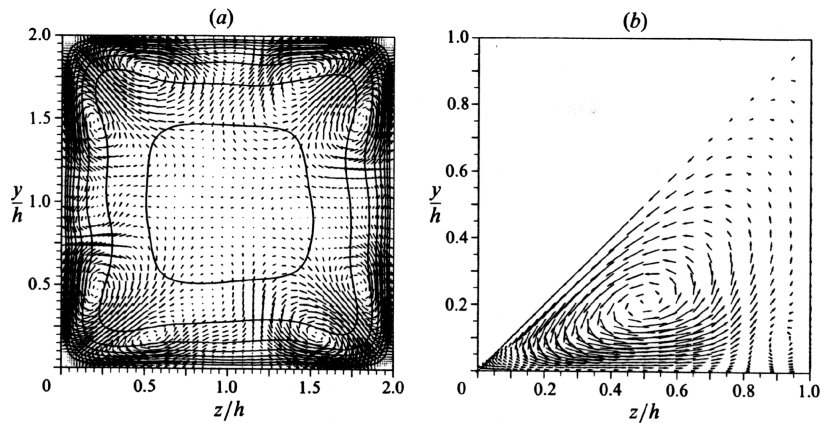
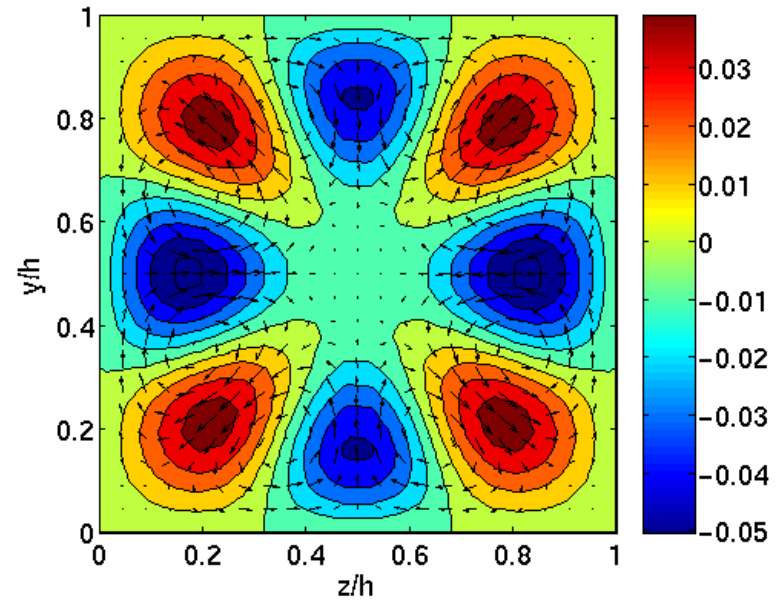


FIGURE 6. (a) Mean secondary velocity vectors and mean streamwise flow contours. The contour increment is $4u$, with the lowest value contour being nearest to the duct walls representing $4u_r$ units. (b) Vector field in (a) averaged over all octants. Only half the vectors in each direction are shown.



DNS, Gavrilakis, *JFM* 1992

unstable TW solution

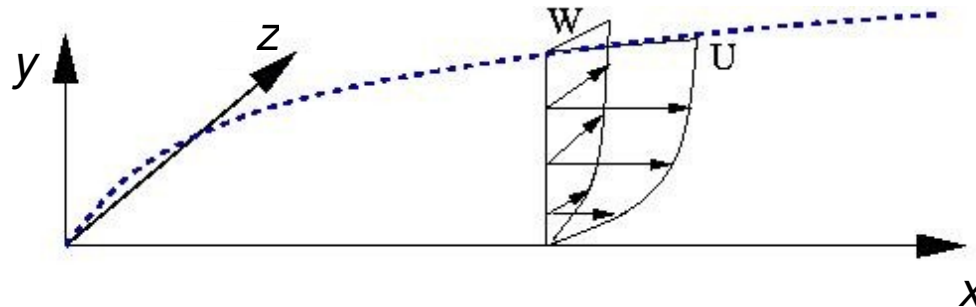


Conversely, the boundary layer presents the difficulty of being **non-parallel** along the streamwise direction x , hence it is not possible to simplify the equations by expanding perturbations in the form:

$$\sum_n f(y,z) e^{i\alpha(x-ct)}$$

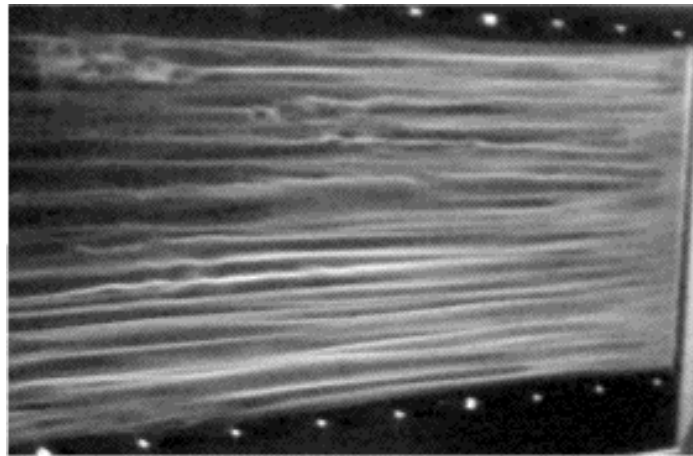
Inflow-outflow conditions?

Proper model and scales for boundary layer streaks/vortices ?





For the time being let's forget about the high frequency TW and let's focus on steady streaks/vortices elongated in x ; the streaks/vortices found will (likely) be **unstable**, and this will be assessed with a subsequent analysis.



Boundary layer scales:
(Görtler-like)

y, z	—————→	$\delta = L Re^{-1/2}$
x	—————→	L
v, w	—————→	$U_\infty Re^{-1/2}$
u	—————→	U_∞
p	—————→	$\rho U_\infty^2 Re^{-1}$

with $Re = U_\infty L / \nu$

(“ p ” above is just the second order term in the usual inner expansion of pressure)



Re-independent steady leading order equations

$$\left\{ \begin{array}{l} u_x + v_y + w_z = 0 \\ (uu)_x + (uv)_y + (uw)_z - u_{yy} - u_{zz} = 0 \\ (uv)_x + (vv)_y + (vw)_z + p_y - v_{yy} - v_{zz} = 0 \\ (uw)_x + (vw)_y + (ww)_z + p_z - w_{yy} - w_{zz} = 0 \end{array} \right.$$

with boundary conditions:

$$\left\{ \begin{array}{ll} u = 0 \text{ at } y = 0 & u = 1 \text{ for } y \rightarrow \infty \\ v = 0 \text{ at } y = 0 & w = 0 \text{ for } y \rightarrow \infty \\ w = 0 \text{ at } y = 0 & p = 0 \text{ for } y \rightarrow \infty \end{array} \right.$$

Streamwise parabolic set of PDE's, leading edge *optimal* conditions can be chosen on the basis of a variational principle:

1. find IC such that the solution at the exit station ($x = L$) (or the solution integrated over x) has a maximum value of the **disturbance kinetic energy**;
17. ... **rate of energy dissipation**;
3. ... **growth rate of the secondary instability (TW)**



At any value of x it is easy to show that u , v and w are constrained through:

$$u v_y + u w_z - v u_y - w u_z + u_{yy} + u_{zz} = 0$$

and if u is uniform along y and z (for example when $u = 1$ uniformly along x , y and z upstream of the leading edge) then the constraint at $x = 0^-$ is simply the continuity equation: $v_y + w_z = 0$

Thus, we need to search only for 2 (!) **optimal** leading edge velocity conditions, the third component being a linear functional of the others.

We decide to fix:

$$\begin{cases} u(0, y, z) = 1 \\ v(0, y, z) = v_0(y, z) \end{cases}$$

(i.e. no streamwise velocity perturbation at the leading edge) and to maximize:

$$G_{\text{mean}} = \frac{E_{\text{mean}}}{E_{\text{in}}} = \frac{(1/(2Z)) \int_{-Z}^Z \int_0^\infty \int_0^1 [|u'|^2 + Re^{-1} (|v'|^2 + |w'|^2)] dx dy dz}{[(1/(2Z)) \int_{-Z}^Z \int_0^\infty [|u'|^2 + Re^{-1} (|v'|^2 + |w'|^2)] dy dz]_{x=0}}$$



Given that Re is “large” we define

$$E_u(x) = \frac{1}{2Z} \int_{-Z}^Z \int_0^{\infty} |u'|^2 dy dz; \quad E_{in} = \left[\frac{1}{2Z} \int_{-Z}^Z \int_0^{\infty} [|v'|^2 + |w'|^2] dy dz \right]_{x=0}$$

so that the functional to be maximed is:

$$\mathcal{J} = G_{\text{mean}} = Re \frac{\int_0^1 E_u(x) dx}{E_{in}}$$

Constrained optimization problem handled with the technique of
Lagrange multipliers

DIFFERENTIATE-THEN-DISCRETIZE vs DISCRETIZE-THEN-DIFFERENTIATE ?
(Gunzburger, **Flow, Turb & Comb.** 2000)



Discretization: second order finite differences on non-uniform grids along x and y , Fourier discretization along z . The direct problem in discrete form can be cast as:

$$\mathbf{A}_{n+1} \mathbf{f}_{n+1} = \mathbf{B}_n \mathbf{f}_n$$

with n the streamwise grid index.

The initial energy can be written as: $E_{\text{in}} = \mathbf{f}_0^T \mathbf{M}_0 \mathbf{f}_0 = E_0$
and the discrete functional is:

$$\mathcal{J} = \sum_{n=1}^N \mathbf{f}_n^T \mathbf{M}_n \mathbf{f}_n$$

Thus the **Lagrangian functional** is:

$$\mathcal{L}(\mathbf{f}_0, \mathbf{f}_n, \mathbf{f}_{n+1}, \mathbf{f}_N) =$$

$$\sum_{n=1}^N \mathbf{f}_n^T \mathbf{M}_n \mathbf{f}_n + \sum_{n=0}^{N-1} [\mathbf{p}_n^T (\mathbf{A}_{n+1} \mathbf{f}_{n+1} - \mathbf{B}_n \mathbf{f}_n)] + \lambda_0 [\mathbf{f}_0^T \mathbf{M}_0 \mathbf{f}_0 - E_0]$$



It is simple to rewrite the Lagrangian functional as:

$$\begin{aligned}\mathcal{L}(\mathbf{f}_0, \mathbf{f}_{n+1}, \mathbf{f}_N) = & \sum_{n=0}^{N-1} \mathbf{f}_{n+1}^T \mathbf{M}_{n+1} \mathbf{f}_{n+1} + \sum_{n=0}^{N-1} [\mathbf{p}_n^T \mathbf{A}_{n+1} \mathbf{f}_{n+1} - \mathbf{p}_{n+1}^T \mathbf{B}_{n+1} \mathbf{f}_{n+1}] \\ & + \mathbf{p}_N^T \mathbf{B}_N \mathbf{f}_N - \mathbf{p}_0^T \mathbf{B}_0 \mathbf{f}_0 + \lambda_0 [\mathbf{f}_0^T \mathbf{M}_0 \mathbf{f}_0 - E_0]\end{aligned}$$

and an extremum is found when the following equation is satisfied:

$$\frac{\mathcal{D}\mathcal{L}}{\mathcal{D}\mathbf{f}_0} \delta\mathbf{f}_0 + \sum_{n=0}^{N-2} \frac{\mathcal{D}\mathcal{L}}{\mathcal{D}\mathbf{f}_{n+1}} \delta\mathbf{f}_{n+1} + \frac{\mathcal{D}\mathcal{L}}{\mathcal{D}\mathbf{f}_N} \delta\mathbf{f}_N = 0$$

for arbitrary variations $\delta\mathbf{f}_0$, $\delta\mathbf{f}_{n+1}$ and $\delta\mathbf{f}_N$



This leads to the following Euler-Lagrange equations:

$$\left\{ \begin{array}{l} \frac{\mathcal{D}\mathcal{L}}{\mathcal{D}\mathbf{f}_0} = -\mathbf{p}_0^\top \mathbf{B}_0 + 2\lambda_0 \mathbf{f}_0^\top \mathbf{M}_0 = 0 \quad \text{optimality condition at } x = 0 \\ \sum_{n=0}^{N-2} \frac{\mathcal{D}\mathcal{L}}{\mathcal{D}\mathbf{f}_{n+1}} = \sum_{n=0}^{N-2} [\mathbf{p}_n^\top \mathbf{A}_{n+1} - \mathbf{p}_{n+1}^\top \mathbf{B}_{n+1} + 2 \mathbf{f}_{n+1}^\top \mathbf{M}_{n+1}] = 0 \\ \frac{\mathcal{D}\mathcal{L}}{\mathcal{D}\mathbf{f}_N} = \mathbf{p}_N^\top \mathbf{B}_N = 0 \end{array} \right.$$

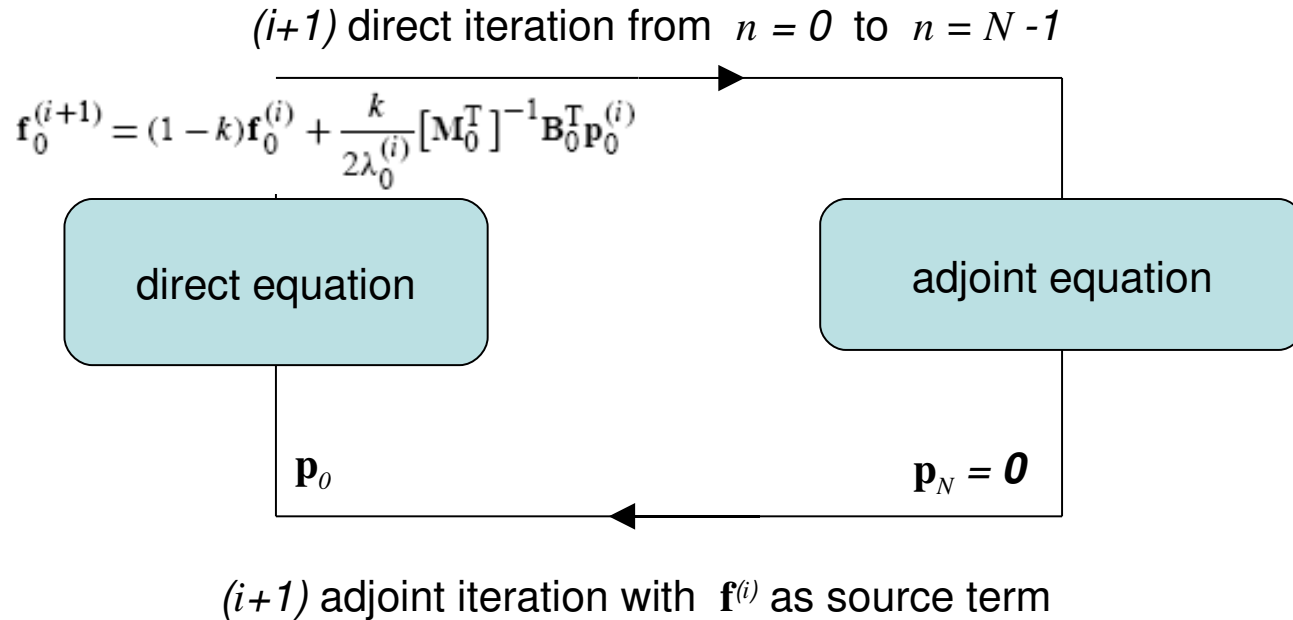
Hence, the *discrete* adjoint problem is

$$\mathbf{A}_{n+1}^\top \mathbf{p}_n = \mathbf{B}_{n+1}^\top \mathbf{p}_{n+1} - 2 \mathbf{M}_{n+1}^\top \mathbf{f}_{n+1}$$

to be solved by marching backward from $x = 1$ to $x = 0$, with the terminal condition $\mathbf{p}_N = \mathbf{0}$.



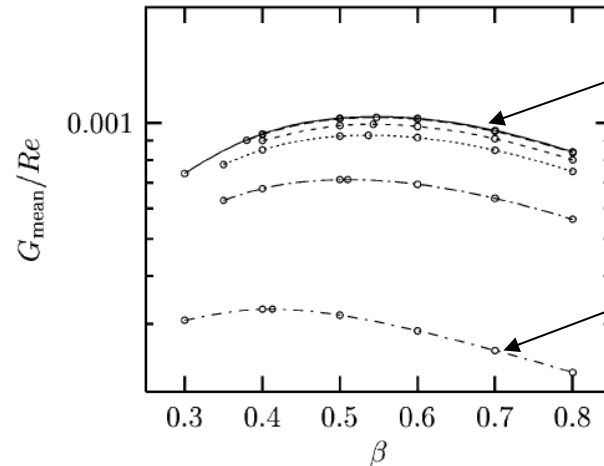
Classical iterative procedure



- The Lagrange multiplier λ_0 is chosen so that the constraint $E_{\text{in}}(\mathbf{f}_0) = E_0$ is satisfied.
- The relaxation parameter $k \in [0, 1]$ allows to relax the **optimality condition** (which is recovered for $k = 1$).
- Iterations are stopped when the objective function converges to the required tolerance.



Mean gain for different initial energy values



$$E_0 = 10^{-7}$$

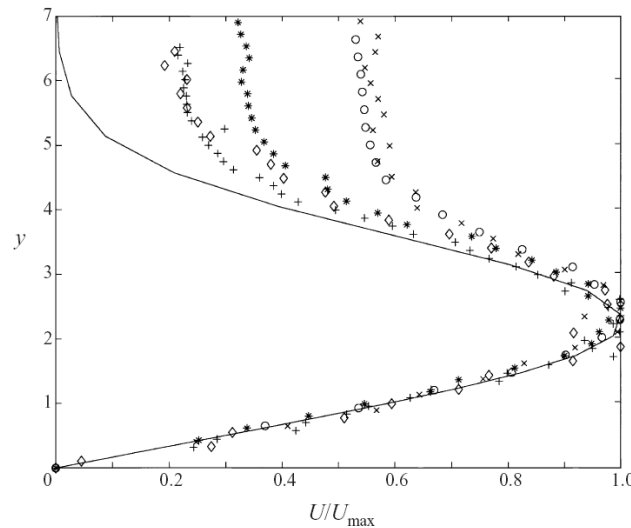
linear result

“optimal perturbations”

$$E_0 = 500$$

very large initial

disturbance amplitude



Comparison between the optimal linear streak and the u_{rms} results by Westin *et al.* (**JFM** 1994)

FIGURE 1. Comparison between the streamwise velocity component of the downstream response to an optimal perturbation, and the u -r.m.s. data in a flat-plate boundary layer subject to free-stream turbulence (—, Reynolds-number-independent theory). The symbols represent experiments from Westin *et al.* (1994) (\circ , $Re_\delta = 203$; $+$, $Re_\delta = 233$; \times , $Re_\delta = 305$; $*$, $Re_\delta = 416$; \diamond , $Re_\delta = 517$). Here y has been made non-dimensional—and the Reynolds number is defined—using the Blasius length scale $\delta = (L\nu/U_\infty)^{1/2}$.

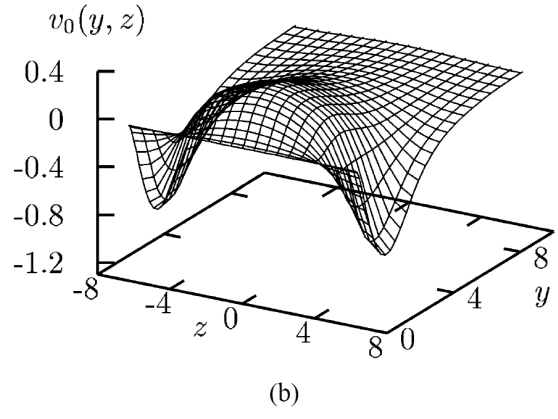
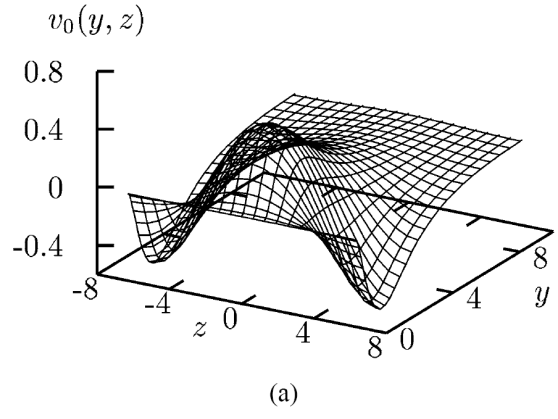


Fig. 5. Surfaces $v_0(y, z)/\sqrt{E_0}$ at fixed wavenumber $\beta = 0.5$ for different E_0 . (a) $E_0 = 1$; (b) $E_0 = 100$.

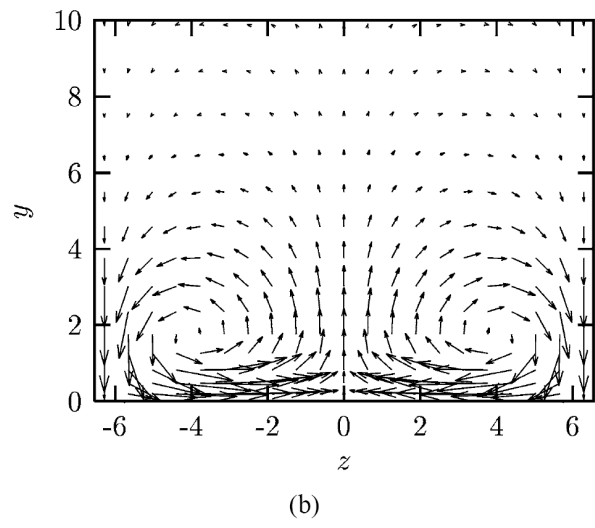
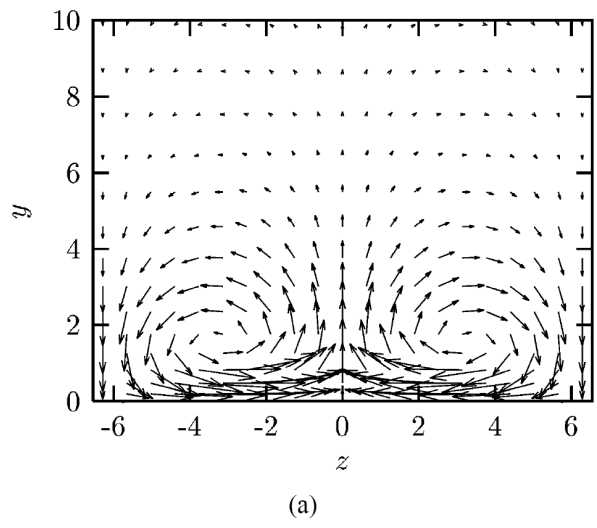


Fig. 6. Disturbance velocity vector plots in the cross-stream plane (y, z) at $x = 0$, for $\beta = 0.5$. (a) $E_0 = 1$; (b) $E_0 = 100$.

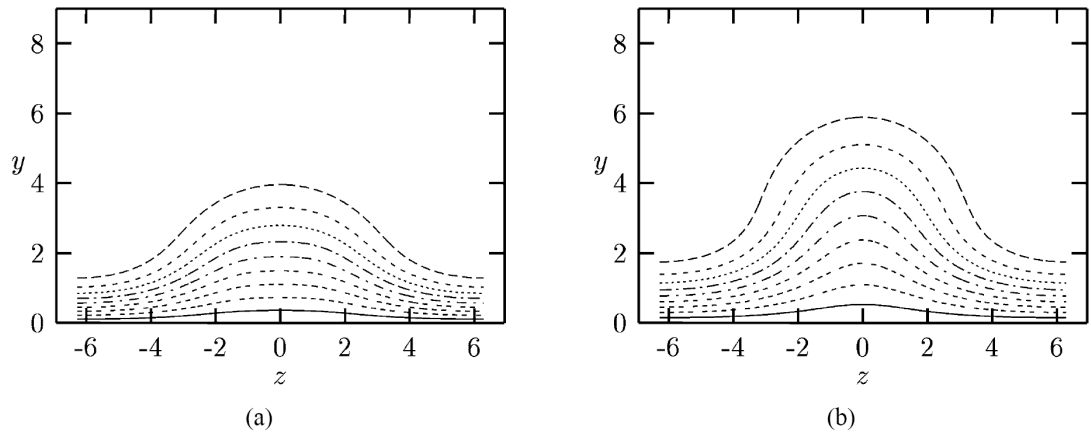


Fig. 7. $\beta = 0.5$, $E_0 = 100$, contours of the streamwise velocity u at: (a) $x = 0.5$, (b) $x = 1$.

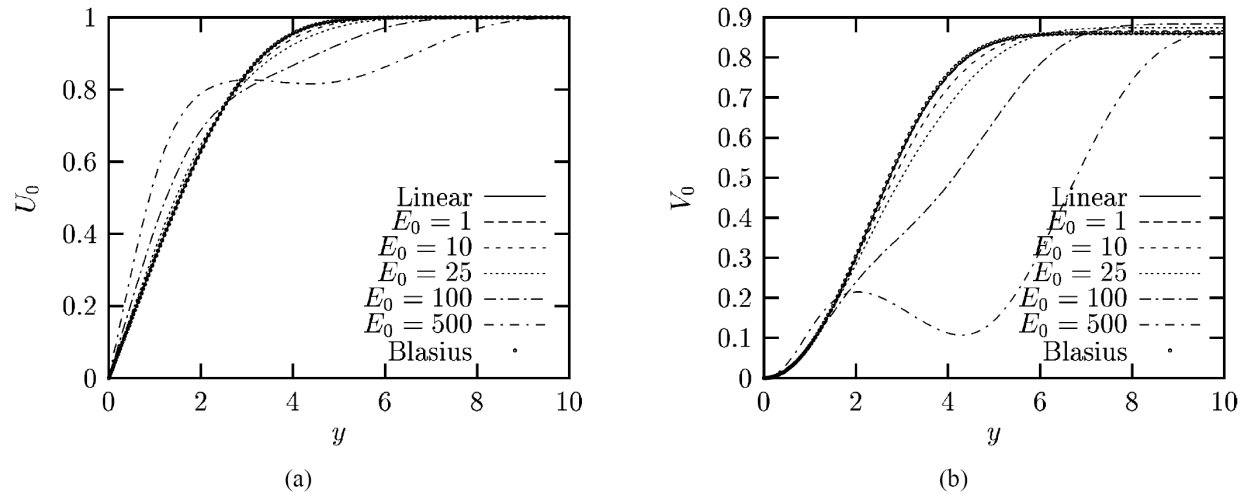


Fig. 8. Comparison at fixed wavenumber $\beta = 0.5$. Mode zero at $x = 1$ for increasing E_0 .

U-velocity profiles are highly inflectional both along y and along z ...



THE BREAKDOWN OF STREAKS: TW SOLUTIONS

The streaks are assumed to evolve slowly compared to the evolution of the “secondary” wavy instability, it is appropriate to focus only on a “parallel” base flow $U(y, z) = \sum_{k=-\infty}^{\infty} U_k(y)e^{ik\beta z}$ (the Blasius flow plus the spanwise periodic streak, neglecting cross-stream velocity components)

and conduct a *local, inviscid analysis*:

$$\left\{ \begin{array}{l} u_x + v_y + w_z = 0, \\ u_t + Uu_x + U_yv + U_zw = -p_x, \\ v_t + Uv_x = -p_y, \\ w_t + Uw_x = -p_z, \end{array} \right.$$

together with slip boundary conditions at the wall and decaying disturbances in the free stream. It is simply to reduce this equation to:

$$\left(\frac{\partial}{\partial t} + U \frac{\partial}{\partial x} \right) \Delta p - 2U_y p_{xy} - 2U_z p_{xz} = 0$$



The disturbance pressure reads: $p(x, y, z, t) = \text{Re} \{ \tilde{p}(y, z) e^{i\alpha(x-ct)} \}$

with $\tilde{p}(y, z) = \sum_{k=-\infty}^{\infty} \hat{p}_k(y) e^{i(k+\gamma)\beta z}$ and $\gamma \in [0, 0.5]$ Floquet exponent.

A temporal analysis is carried out (c eigenvalue, α real wave number) separating the solutions according to the possible symmetries:

sinuous or varicose instabilities

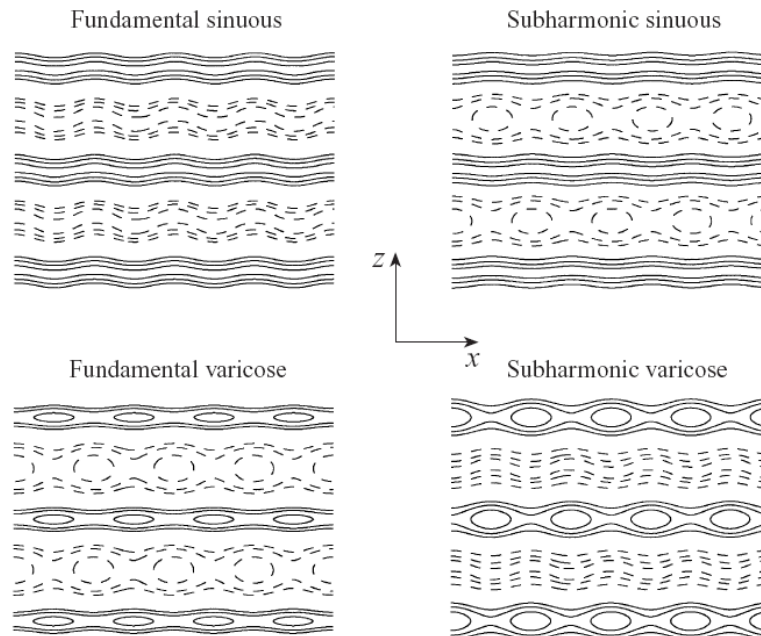


FIGURE 2. Sketch of streak instability modes in the (x, z) -plane over four streamwise and two spanwise periods, by contours of the streamwise velocity. The low-speed streaks are drawn with solid lines while dashed lines are used for the high-speed streaks.



Inviscid stability results

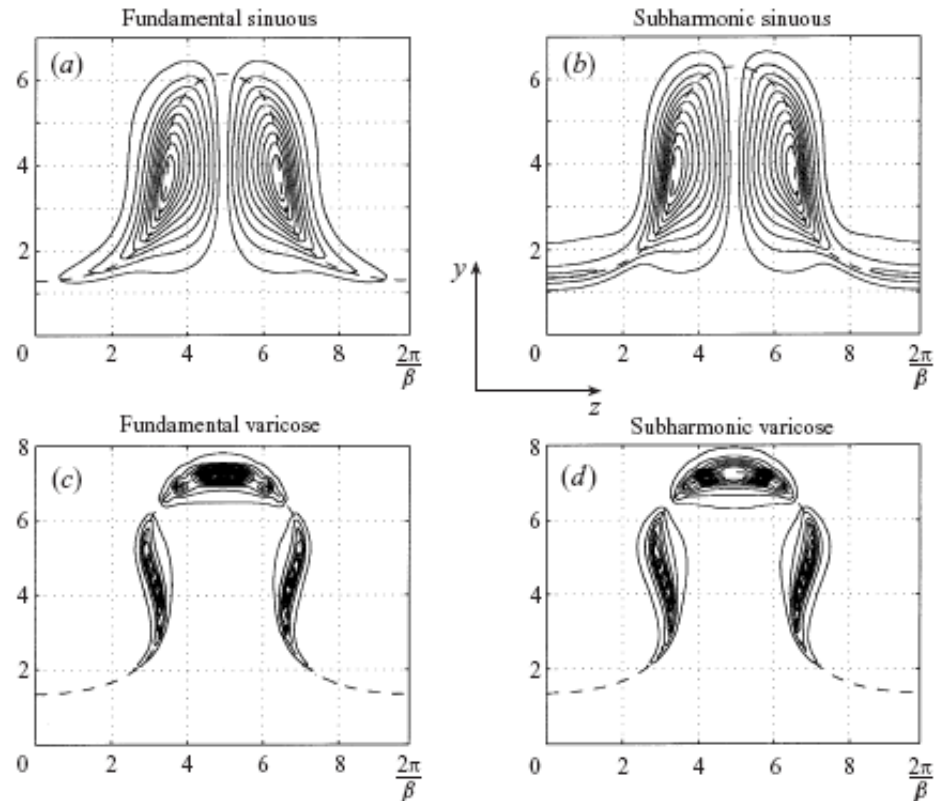


FIGURE 12. Contours of constant absolute values of the streamwise velocity component of four different kinds of modes obtained using the nonlinear mean fields. The dashed lines represent the contours of the constant value of the mean field corresponding to the phase velocities of the disturbances. The sinuous modes are calculated using the nonlinear mean field corresponding to the circled line in figure 5(a), at streamwise position $x = 2$, where $A = 0.36$, for a streamwise wavenumber $\alpha = 0.280$ ($c_r = 0.821$ and $\omega_i = 0.0144$ for the fundamental mode; $c_r = 0.839$ and $\omega_i = 0.0125$ for the subharmonic mode). The varicose modes are calculated using the mean field with largest streak amplitude (see figure 5b) at position $x = 2$, where $A = 0.378$, for a streamwise wavenumber $\alpha = 0.275$ ($c_r = 0.866$ and $\omega_i = 0.00218$ for the fundamental mode; $c_r = 0.876$ and $\omega_i = 0.00243$ for the subharmonic mode). In all calculations $Re_\delta = 430$ and $\beta = 0.45$.



Effect of detuning

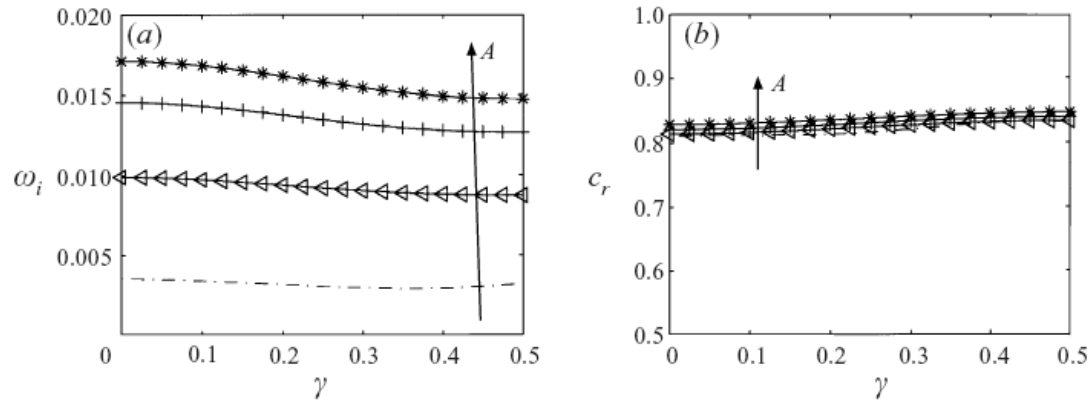


FIGURE 17. Temporal growth rate (a) and phase speed (b) versus the Floquet parameter for sinusous modes, for four different amplitudes of the primary disturbance (symbols as in figure 16).

Constant growth curves

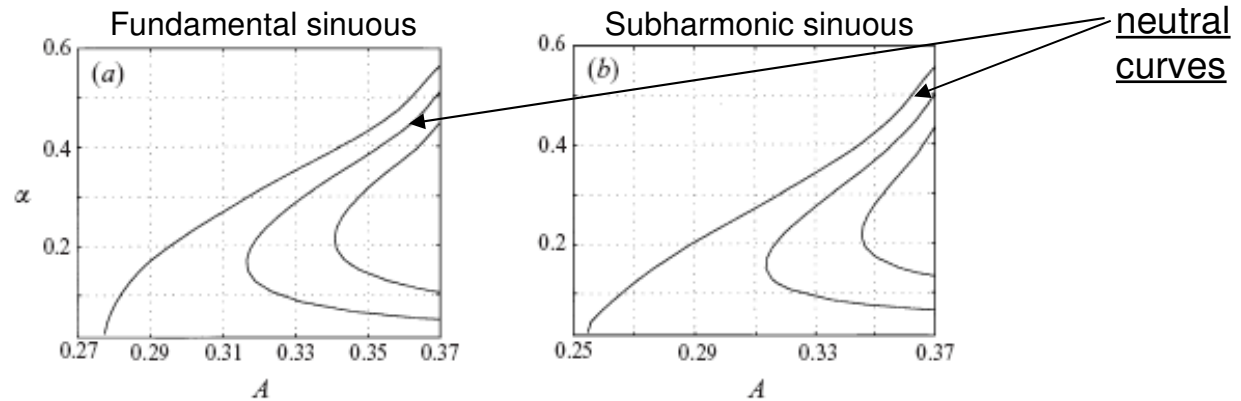


FIGURE 19. Neutral curves for streak instability in the (A, α) -plane for (a) the fundamental sinusous mode, (b) the subharmonic sinusous mode (contour levels: $\omega_i = 0, 0.0046, 0.0092$).



To provide a conservative estimate of the *threshold amplitude* of the initial disturbance at $x = 0$ that eventually leads to streaks that can break down, we take a “critical” amplitude of the nonlinear streaks A equal to 20%, with $A = A(x; E_0, \beta)$, we can, for each given saturation value of A and for each β , retrieve the corresponding initial energy level E_0 . In a real physical situation the initial energy level capable of yielding the given value of A at saturation will be larger, since leading edge conditions in a wind tunnel are not optimal (in the sense considered here) \Rightarrow *conservative bound*

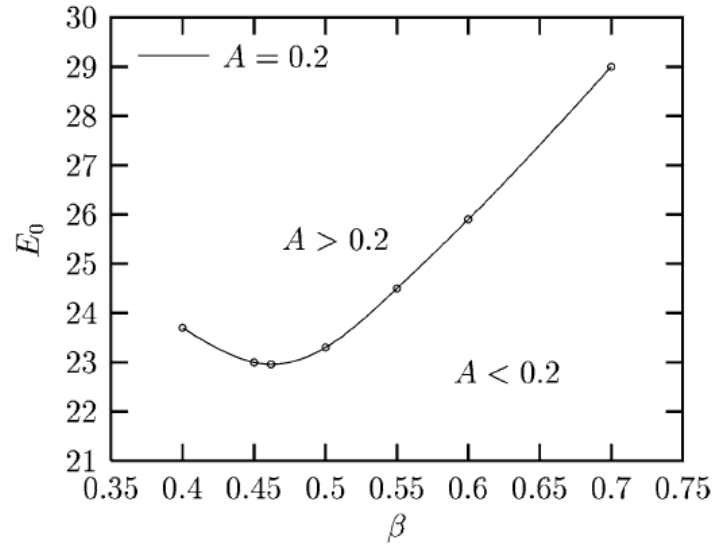


Fig. 12. Curve of initial perturbation energy E_0 as a function of β for which $A = 0.2$ somewhere in the domain.



It can be argued that for initial disturbance energies E_0 at $x = 0$ lower than about **23** (a value which needs to be further divided by Re to yield a physically relevant number) the threshold amplitude needed to trigger an instability of the streaks is not met. In this case



no streaks breakdown nor *by-pass* transition (?)



no self-sustained process



Outlook and conclusions

- Optimal **nonlinear** streaks have been computed in a non-parallel boundary layer by a variational technique which relies on direct-adjoint iterations
- Streaks considered are steady and streamwise elongated → no “short” TW ...
- The cost functional used is *loosely* related to the “secondary” instability of the streaks (possibly a “better” functional could be adopted)
- A locally parallel, inviscid secondary stability analysis has been conducted to assess the potential of initial disturbances to produce downstream flow states with TW
- It appears that a minimal initial disturbance energy $E_o = 23/Re$ is required for the possible onset of TW
- Put **vortices**, **streaks** and **TW** together in a unique variational formulation is not simple, but it is indispensable to capture *vortical states*
(is DNS the only way to go?)